Can convolution and deconvolution be used as tools for modeling multi-component, mixing-limited reaction networks?

Nicholas B. Engdahl[1], James L. McCallum[2], and Timothy R. Ginn[1]

[1]Civil and Environmental Engineering,

Washington State University, Pullman, WA,

USA

[2]School of Earth Sciences, University of

Western Australia, Crawley, WA, Australia

Abstract. Transfer functions (*i.e.* convolutions) have been powerful tools for both forward modeling and reconstructing past states of transport systems in a wide range of subsurface flow problems. The advantage of the transfer function is that it is a simple alternative to complicated, distributed parameter models of flow and transport, but the majority of applications of transfer functions in hydrology have been limited to relatively simple cases, like passive tracers or first-order decay. The central question evaluated in this note is whether or not multi-component mixing limited reactive transport can be represented within a transfer function framework. Our examples consider forward-in-time (FIT) predictions, and backward-in-time (BIT) reconstructions of a carbonate system that represents the intrusion of sea-water into a freshwater aquifer. The main result is that accurate FIT and BIT models are developed by posing the problem in terms of conservative components. As with all convolution-based methods, the results are sensitive to errors and/or noise in the input functions, but we show that smoothed approximations of the requisite functions provide good representations of transport. Given the vast unknowns in any subsurface transport problem, such generalized, reactive transfer function models may have yet unexplored advantages when the tradeoffs between overall computational cost, accuracy, and uncertainty are explored in more detail.

1. Introduction

Transfer functions have seen widespread use across the diverse spectrum of hydrogeologic applications ranging from simulating solute dispersion [e.g., *Jury*, 1982; *Simmons*, 1982], to upscaling aquifer reactivity [*Seeboonruang and Ginn*, 2006; *Loschko et al.*, 2016], among numerous other applications. The mathematics of transfer functions are reviewed in section 2, but the basic concept is that a response function is used to filter an input signal and the resulting output models solute arrivals in terms of a breakthrough curve. Analogous nomenclature include convolutions, streamtube ensembles, or stochastic-convective models, but in each case the idea is to use the "characteristic response" of the porous media to model transport in-lieu of solving complex, spatially heterogeneous, partial differential equations. The response function can be obtained directly from data (natural tracers or tracer tests), inferred from other models, or estimated stochastically, but, regardless of the source, transfer functions have provided a conceptually simple, and computationally fast method for accurately modeling the transport of simple tracers.

Transfer functions have seen extensive use for approximating passive transport and for inferring residence time distributions (RTDs) from multiple environmental tracers [*Cook and Böhlke*, 2000]. The latter often involves a combination of forward-in-time (FIT) and backward-in-time (BIT) modeling to reconstruct input concentrations of different chemical constituents like chlorofluorocarbons or radiogenic tracers, sometimes with sorption [*Cvetkovic et al.*, 1998]. Applications where multi-component reaction systems have been modeled with transfer functions [e.g. *Cirpka and Kitanidis*, 2000; *Ginn*, 2001; *Botter et al.*, 2005] are less frequent. However, some examples where this could be beneficial

include bioremediation [e.g. *Cirpka and Kitanidis*, 2001; *Luo et al.*, 2008], including transient flows [e.g. *Ginn et al.*, 2001; *Sanz-Prat et al.*, 2015], and estimation of groundwater nitrate levels [*Alikhani et al.*, 2016] or denitrification rates [*Green et al.*, 2016, 2018]. The challenge is that many reactive transport problems are mixing limited [e.g. *Chiogna et al.*, 2011; *Dentz et al.*, 2011] and it is often not straightforward to accurately model multi-component mixing with transfer functions, although some headway has been made [e.g. *Luo and Cirpka*, 2008; *Sanz-Prat et al.*, 2015].

Multi-component systems are typically simulated using numerical distributed parameter models (DPMs) that explicitly model transport, mixing, and reactions. DPMs have become increasingly detailed in recent years so that coupled transport and multi-component chemical reaction processes can be represented simultaneously [e.g. *Steefel and Lasaga*, 1994; *Prommer et al.*, 2003; *Parkhurst et al.*, 2004]. The high amount of process-level realism makes these DPMs powerful tools, but the degrees of freedom in these models are immense and come with a high computational cost. DPMs have evolved to the point where they now require a supercomputer to simulate realistic systems at reasonable spatio-temporal resolutions [see *Hammond et al.*, 2014; *Beisman et al.*, 2015; *Gardner et al.*, 2015]. The long runtimes also make it difficult to assess parameter sensitivities, quantify time step integration errors, investigate uncertainties, or to perform a grid-convergence analysis, which are necessary steps for robust, predictive models.

DPMs are without question immensely valuable tools, but the hurdles presented by DPMs and their calibration has led to the search for effective upscaling methods mixing-limited reactive transport systems. Here we suggest a top-down approach and posit that transfer functions applied at the field scale may offer a computationally efficient, rel-

atively unexplored alternative to DPMs for complex reactive transport systems. This note provides a demonstration of how to incorporate complex, multi-component reaction networks into transfer function models, in both forward and backward problems, using convolution and deconvolution, respectively. We show how careful consideration of the chemical species and the reaction network allows simplification of the reaction network using conservative components, and the transport of these components can be modeled with transfer functions. Our example problem considers the reactive transport of seawater intruding into a freshwater aquifer, and we show that these simplified models provide good approximations of the systems' dynamics. Our main point is that transfer functions and conservative components can be a conceptually simple alternative to DPMs for estimating multi-component transport, which may have untapped potential for diverse transport problems.

2. Mathematical background

This section provides a brief overview of the basic properties of convolution and deconvolution, including the necessary real-space and Laplace/Fourier space properties, and some analytical examples. Readers that are already familiar with these concepts may skip to section 3 where the multi-component geochemical system is introduced.

2.1. Convolution is a forward operator in time

Linear transfer functions are common throughout hydrology, with applications to transport, residence time, and environmental tracer interpretations [*Małoszewski and Zuber*,

1982; *Cook and Böhlke*, 2000]. One of the the most general forms is:

$$c(t|x) = \int_0^\infty f(t-\tau)\exp(-\lambda\tau)g(\tau|x)d\tau \tag{1}$$

where $c(t|x)$ is an observed concentration, conditional to the sampling location x, $f(t)$ is an input function, λ is a first-order decay rate, and $g(t|x)$ is the Green's function of transport in the system, which is also the travel time distribution (TTD) [modified from *Simmons et al.*, 1995]. Note that the strictest definition of a "Green's function" implies a solution of a partial differential equation; however, it may not be possible to write an accurate PDE for natural systems, so we adopt the more liberal definition of "a characteristic response" of any system to a instantaneous, unit input. Equation (1) is an integrated response model because it does not directly consider spatial changes, but the nature of the Green's function allows this to represent subsurface flows [e.g. *Jury*, 1982; *Ginn*, 2001], and/or watersheds [e.g. *Kirchner et al.*, 2001; *Harman et al.*, 2010; *Benettin et al.*, 2013].

Convolutions offer a simple, but accurate, framework for modeling transport in any system that can be conceptualized as a single reservoir, or as a series of reservoirs that feed into each other [*Sardin et al.*, 1991]. Some important properties can be shown by defining a generic $g(t|x)$ to represent the Green's function from an inlet to some observation location at $x = L$ $[L]$. Convolutions may be applied sequentially and this allows one to build complex problems from a collection of simpler ones, and even to decompose a non-stationary domain into a series of stationary domains. Instead of constructing the breakthrough curve (BTC) for transport from $x = 0 \rightarrow L$, the problem can be divided into two, or more parts, each spanning part of the domain. For example, use two sections where $\alpha + \beta = L$, $(\alpha, \beta > 0)$. The system can now be described by two transfer functions.

The first represents transport from $x = 0 \rightarrow \alpha$ and uses the input function $f(t)$ to generate $c(t|x_{[0,\alpha]})$, where $x_{[0,\alpha]}$ is used as shorthand to denote the endpoints of the transport problem. The second transfer function represents transport from $x = \alpha \rightarrow L$. This uses $c(t|x_{[0,\alpha]})$ as the input function to generate $c(t|x_{[\alpha,L]})$.

A convenient analytical form is obtained by taking the Laplace transform (LT) of Eq. (1) (with $\lambda = 0$ for simplicity):

$$\tilde{c}(s|x_j) = \tilde{f}(s)\tilde{g}(s|x_j) \tag{2}$$

where $\tilde{*}$ denotes a LT function ($*$ is used here as a placeholder) and the Laplace variable s is the dual to time ($t \rightarrow s$). Using this notation and substituting, the two transfer functions are:

$$\tilde{c}(s|x_{[0,\alpha]}) = \tilde{f}(s)\tilde{g}(s|x_{[0,\alpha]}) \tag{3a}$$

$$\tilde{c}(s|x_{[\alpha,L]}) = \tilde{c}(s|x_{[0,\alpha]})\tilde{g}(s|x_{[\alpha,L]}) \tag{3b}$$

Inserting the right hand side of (3a) into (3b) one finds:

$$\tilde{c}(s|x_{[0,L]}) = \tilde{f}(s)\tilde{g}(s|x_{[0,\alpha]})\tilde{g}(s|x_{[\alpha,L]}) \tag{4}$$

which highlights the sequential nature of these operations. The same could be shown in the time domain by sequential application of (1), but (2) is more compact.

2.2. Deconvolution is the backward time operator

Conceptually, deconvolution is the inverse operator of convolution similar to the way that $\ln[x]$ is the inverse of $\exp[x]$, but deconvolution is for arbitrary functions and is technically the "un-filtering" of a convolution. Discrete deconvolutions have been used to reconstruct residence time distributions from environmental tracers [*Cirpka et al.*, 2007;

McCallum et al., 2014], and continuous deconvolutions also have demonstrated their utility, even in highly heterogeneous [*Fienen et al.*, 2006; *Engdahl et al.*, 2013], or transient systems [*Liao et al.*, 2013]. The approach has also been applied successfully to the interpretation of tracer tests in streams [*Payn et al.*, 2008; *Gooseff et al.*, 2011] and theoretically to transport in heterogeneous sediments [*Luo and Cirpka*, 2008]; note that most studies involving deconvolution are limited to passive tracers or 1st-order (decay) reactions, which are representative of the literature overall.

Consider (3a) in the context of a deconvolution. Given an observed concentration function, $c(t)$, and a known input function, $f(t)$, the travel time distribution (Green's function) can be found as:

$$\tilde{g}(s|x_{[0,\alpha]}) = \tilde{c}(s|x_{[0,\alpha]}) \left[\tilde{f}(s)\right]^{-1} \tag{5}$$

Inverting the Laplace transform then directly recovers the Green's function. If one wishes to reconstruct an input function instead, the only change required is algebraic:

$$\tilde{f}(s) = \tilde{c}(s|x_{[0,\alpha]}) \left[\tilde{g}(s|x_{[0,\alpha]})\right]^{-1} \tag{6}$$

The simplest way to verify this analytically is to define an exponential Green's function, $g(t) = \exp(-\gamma t)$, where $\gamma > 0$ is some constant, and a Dirac-delta for the input function, $f(t) = \delta(t)$, so that $c(t) = \exp(-\gamma t)$; using any two of these easily invertable functions the third can be recovered exactly from (5) or (6). Similar results can be shown for any combination of input and Green's functions. For example, if the output function is known to be $c(t) = \exp(-\eta t)$ (requiring $\eta > 0$), we can use our exponential $g(t)$, and solve for an unknown input function. Taking the LT of $g(t)$ and $c(t)$ and inserting these into (2)

we find:

$$\frac{1}{s+\eta} = \tilde{f}(s)\frac{1}{s+\gamma} \tag{7a}$$

$$\tilde{f}(s) = \frac{s+\gamma}{s+\eta} \tag{7b}$$

$$f(t) = (\gamma - \eta)\exp(-\eta t) \tag{7c}$$

If (7c) and $g(t)$ are substituted into (1), or (2), it can be shown that this $f(t)$ recovers $g(t) = \exp(-\gamma t)$. These "closed loop" validation exercises, where various components of the problem are omitted, emphasize the fact that any two pieces of information needed for (1) can be used to find the third. This property enables reconstruction of concentration histories, not just forward modeling, but so far nothing beyond first-order decay has received rigorous treatment in the literature.

3. Multi-component, mixing limited reactive transport

The purpose of this note is to demonstrate how transfer functions can be applied to multi-component reaction networks. The geochemical system we consider is the textbook carbonate system. The four aqueous, equilibrium reactions are:

$$HCO_3^- = H_2O + CO_{2(aq)} - H^+ \tag{8a}$$

$$CO_3^{2-} = H_2O + CO_{2(aq)} - 2H^+ \tag{8b}$$

$$Ca^{2+} = CaCO_3 - CO_{2(aq)} - H_2O + 2H^+ \tag{8c}$$

$$OH^- = H_2O - H^+ \tag{8d}$$

and the equilibrium constants for these reactions are $\log[K_1] = 6.3447$, $\log[K_2] = 16.6735$, $\log[K_3] = -8.1934$, and $\log[K_4] = 13.9951$, respectively (note that these are base-10 logarithms by convention). The problem is simplified by identifying a secondary species

for each reaction and using the equilibria laws of mass action to express each secondary in terms of the remaining two primary species, $CO_{2(aq)}$ and H^+, as:

$$\log \boldsymbol{c}'' = \mathbf{S} \log \boldsymbol{c}' - \log \mathbf{K}^* \tag{9}$$

where $\boldsymbol{c}'' = [c_{HCO_3}, c_{CO_3^{2-}}, c_{Ca^{2+}}, c_{OH^-}]^{\mathrm{T}}$ is the vector of secondary species concentrations, $\boldsymbol{c}' = [c_{CO_2}, c_{H^+}]^{\mathrm{T}}$ is the vector of primaries, $\mathbf{S}$ is a stoichiometry matrix (Appendix A), and $\mathbf{K}^*$ is the vector of equilibrium constants, adjusted for ionic strength impacts on the activity coefficients (Appendix A).

The reactive transport problem is an end-member mixing situation described by *de Simoni et al.* [2007] where we assume an aquifer has an initial concentration of $CO_{2(aq)} = 3.4 \times 10^{-4}$ and $pH = 7.3$, with an ionic strength of $I_s = 5.0 \times 10^{-3}$; this solution is denoted as "end-member A," abbreviated EM-A. We assume as intrusion of seawater into the aquifer that has initial concentration of $CO_{2(aq)} = 3.51 \times 10^{-4}$ and $pH = 7.16$ and an ionic strength of $I_s = 6.25 \times 10^{-1}$; this solution is denoted as EM-B. A mixture of these end-member waters creates a multi-component chemical equilibrium state that could be solved with programs like PhreeqcRM [*Parkhurst and Wissmeier*, 2015] or CrunchFlow [*Steefel and Lasaga*, 1994], but here we take an analytical alternative.

3.1. Components and mixing ratios

We follow *de Simoni et al.* [2007] (and many others) to simplify our carbonate problem by adopting conservative components. Components are common tools in the mixing and reactive transport literature, but they have not seen widespread use elsewhere in hydrogeology. The idea is to linearly combine the transport and reaction equations for each chemical species in such a way that reactions are eliminated. For the system defined

by (8), these components can be defined as:

$$u_1 = CO_2 + HCO_3^- + CO_3^{2-} - Ca^{2+} \tag{10a}$$

$$u_2 = H^+ - HCO_3^- - 2CO_2 + 2Ca^{2+} - OH^- \tag{10b}$$

where the molecular formulas represent the concentration of each species. The convenience of these components is that they are conservative and so their transport equations include no equilibrium reactions. Given observed values of the primary and secondary species, one can compute the values of the conservative components u_1^* and u_2^*, where the $*$ indicates this as a derived (mixture) value. When it is not at an end-member, the observed values of u_i^* represent a mixture of the two known end-member concentrations, $u_{i,A}$ and $u_{i,B}$ respectively, but the nonlinear speciation problem must be solved to determine individual concentrations. Denoting the fraction of EM-B as α, the contribution of EM-A must be $1 - \alpha$, so α may be found by solving either:

$$u_1^* = (1 - \alpha)u_{1,A} + \alpha u_{1,B} \tag{11a}$$

$$u_2^* = (1 - \alpha)u_{2,A} + \alpha u_{2,B} \tag{11b}$$

de Simoni et al. [2007] term α fraction as the "mixing ratio," which evolves analogously to a conservative tracer. In the context of (1), we can use u_i^* as the transported quantity for $c(t|x)$ (with appropriate input functions) instead of modeling individual solutes, which could not be done in this case since all the solutes of concern are reactive. Since the u_i^* are computed from the mixing ratio, all that is needed for the model is a time series of α and the mass action laws defined by (8) and (10). This information allows elimination of CO_2 from the system of equations. Doing so leaves only H^+, which can be found given

values of u_i^*, then we can recursively solve for CO_2 (Appendix A). This completes $\boldsymbol{c}'$, so (9) gives the remainder of the solution.

This approach has the advantage of eliminating the reactions from the transport equations [e.g. *Steefel and MacQuarrie*, 1996; *Bethke*, 2007]. When used in conjunction with mixing ratios, primary and secondary species concentrations are only computed when needed at specific locations or times [*de Simoni et al.*, 2007], and the transport of the components u_1 and u_2 are conservative, so there is minimal computational overhead. The complete geochemistry now depends only on the mixing ratio, α, and the entire system is now simple enough that it can be represented with a single, passive transfer function model; components have allowed us to greatly simplify the solution technique without simplifying the problem. We refer readers to Appendix A and also to *Ginn et al.* [2017] for additional details and minor corrections to the approach of *de Simoni et al.* [2007].

3.2. Reference model setup

Three kinds of models are used in this note so to avoid confusion we use adopt the following conventions. The "reference" models are those generated via Random Walk Particle Tracking (RWPT) simulation and *are limited to chemical data*; this includes all the species in carbonate system and the first-order tracers used to infer travel times, but we emphasize that no TTDs are generated numerically. Transport is simulated from an inlet to three observation sites (monitoring wells), denoted A, B and C, in order of increasing distance from the inlet (positions defined below). The "forward" models will use the observed time series at site A to simulate the concentrations at B and C, and the "backward" models will use the observations from C and B to reconstruct concentrations at B and A, respectively, providing a third length scale for our evaluation.

Our transport problem considers a pulse of water with a high fraction of seawater entering a freshwater aquifer, which might represent infiltration from a levee or sea-level rise. The domain is a relatively homogeneous aquifer of dimensionless length $L = 25[L]$ with a mean velocity of $v = 2.5 \times 10^{-2}[L/T]$ length and a hydrodynamic dispersion coefficient of $D = 1.0 \times 10^{-1}$, giving a Peclet number of 6. The forward model is simulated with a single realization RWPT model to add random noise to the system, and the three transport distances from the inlet are: $x = [6.25,\ 12.5,\ 25.0]$, for sites A, B, and C, respectively. The forward model uses a high-resolution, implicit operator splitting scheme to simulate the equilibrium geochemical system [*Engdahl et al.*, 2017]. Additionally, two first-order decaying tracers were simulated, which represent ^{39}Ar and ^{3}H, for the purpose of estimating TTDs in section 4.1. The quantity of interest for these transfer function models is the mixing ratio, α, over time at each control point; these were calculated from the reference model's chemical data and are shown as the solid curves in Figure 1. Lastly, we note that artificial errors were not added to these results because the RWPT model has already added noise that deviates from smooth analytical models; however, some notes on the impact of errors in the chemical datasets is included in our discussion.

4. Evaluation of the transport models

Our example considers the performance of the component based solution scheme for the FIT and BIT reactive transport problems. In general, the approach is to first estimate TTDs between the observation site and the target site from tracers, build the mixing ratio function(s) over time, use convolution/deconvolution to propagate $\alpha(t)$, then solve the geochemical speciation problem from the estimated time series of α.

4.1. Building $g(t)$ from radiometric tracers

Estimates of the TTDs ($g(t)$) are needed in order to apply transfer functions as propagators. Given a basic knowledge of the aquifer (*i.e.* weakly heterogeneous), we assume an inverse Gaussian (IG) distribution, which is also a good choice for any confined aquifer in the absence of other information [*Ginn et al.*, 2009; *Engdahl and Maxwell*, 2014]. A two parameter form of the IG can be found in *Massoudieh and Ginn* [2011]:

$$g(p_1, p_2, t) = \frac{p_2}{\sqrt{p_1 \pi t^3}} \exp\left[\frac{-(t-p_2)^2}{p_1 t}\right] \tag{12}$$

In terms of transport parameters, p_1 and p_2 correspond to

$$p_1 = \frac{4D^*}{(v^*)^2} \tag{13a}$$

$$p_2 = \frac{x_i}{v^*} \tag{13b}$$

where $*$ denotes an estimated or "effective" value.

The forward and backward models use the data-driven methods outlined by *Massoudieh and Ginn* [2011] and *Engdahl* [2014] to estimate the TTDs from the inlet to points A,B, and C, then use deconvolution to generate the TTDs between each observation location [see *Engdahl and Maxwell*, 2014]. These methods can provide accurate approximations of TTDs, even in heterogeneous media.

The parameters of (12) can be found from a single observation well when the steady-state concentrations of two radiometric tracers with different half-lives are known. This estimate is only valid at the sampling well, but no *a priori* knowledge of D^* or v^* is

needed:

$$p_1 = \frac{4}{\lambda_2}\frac{\omega_1}{\omega_2}\left(\frac{\omega_1}{\omega_2} - 1\right)\left(\frac{\lambda_1}{\lambda_2} - \frac{\omega_1}{\omega_2}\right)\left[\frac{\lambda_1}{\lambda_2} - \left(\frac{\omega_1}{\omega_2}\right)^2\right]^{-2} \tag{14a}$$

$$p_2 = \frac{\omega_1}{\lambda_2}\left(\frac{\omega_1}{\omega_2} - 1\right)\left[\frac{\lambda_1}{\lambda_2} - \left(\frac{\omega_1}{\omega_2}\right)^2\right]^{-1} \tag{14b}$$

where $\omega_i = \ln(c_i)$ and λ_i corresponds to the first-order decay rate of the ith tracer [*Massoudieh and Ginn*, 2011]; note that two tracers with different non-zero decay rates are required. Equation (14) can be used directly to create a TTD from observed c_i and (12), but it can also be used to estimate the transport parameters. Measurements from two different observation wells will directly give two different values of p_2, so, as long as the distance *between* the observation wells, *e.g.* $x_2 - x_1$, is known, v^* can be estimated; either value of p_1 can then be used to recursively compute D^*. Note that this approach can be sensitive to errors, but large measurement errors would be needed to impact the log-transformed ω_i [*Engdahl and Maxwell*, 2014].

Based on these equations, we can estimate p_1 and p_2 at each location, and back calculate D^* and v^*; the reference model concentrations are given in Table 2. Averaging the estimated values from each well, we found $D^* \approx 1.0 \times 10^{-1}$ and $v^* \approx 2.5 \times 10^{-2}$ for the system, which agree well with the real values. The estimated TTDs are shown in Fig 1 as the black dashed lines, which are smoothed but reasonable approximations of the actual TTDs. The known distances between the wells then allows generation of the $g(t)$ functions between each well (via 5 and 6), which are the TTD approximations needed for the FIT and BIT models. A key point is that the distance from the source to the observation wells is not necessary unless one is reconstructing the source; we do not do so here but

this TTD could also be estimated from D^* and v^*; the emphasis being "estimate," which we discuss further in section 5.

4.2. Forward modeling

Two examples of forward (FIT) modeling with transfer functions are shown: a predictive model from site A to B, and also from A to C. We use time series observations of the ionic strength, pH, and the following chemical concentrations from the reference model: ^{39}Ar, ^{3}H, CO_2, HCO_3^-, CO_3^{2-}, Ca^{2+}, OH^- (values given in Table 1). The tracers ^{39}Ar and ^{3}H were already used to estimate the TTDs, but the other species are used to directly compute u_1^* and u_2^*. The mixing ratio, $\alpha_i(t)$, where i indexes the observation locations (here site A), is the found by solving (11) and this provides all the required information. The convolution(s) are evaluated using (2) where $\alpha_A(t)$ is used as the input function, $f(t)$, for both examples, and we use the Fast Fourier Transform (FFT) its inverse (IFFT) that are built in to the Matlab programming environment for the numerics. The TTDs, $g_{A-B}(t)$ and $g_{A-C}(t)$ are generated from (12) using D^* and v^*, with $x_{A-B} = x_B - x_A$ and $x_{A-C} = x_C - x_A$ for the distances, respectively. The constant temporal discretization of the time series was $dt = 3[T]$, over the time interval $t = 0 \rightarrow 6000$ (2000 samples); finer discretization had a negligible impact on the results. Once the estimated mixing ratio function is generated for B and C, the primary species are found following Appendix A, then used in (9) for the full speciation.

The results of the FIT models are shown in Figure 2a for the mixing ratios and Figure 3a, c, and e for selected chemical species. Focusing on α (Fig 2a), the estimated curves, B_{model} and C_{model}, are good approximations of the "true" reference models, and the mean squared relative error for the mixing ratio functions were on the order of 10^{-3}. The RWPT

noise is not retained in the FIT models but this is typical of convolutions since they are "smoothing" filters. Inspecting the chemical species in Figure 3, similarly good agreement is observed for all the FIT models. This shows that the FFT/IFFT pair is an effective tool for rapidly approximating forward convolutions, and we also found that it is minimally sensitive to the temporal resolution; decreasing the number of sample points to as few as 300 gave similar results, though some errors in the early time chemical data began to grow.

4.3. Backward modeling

The BIT examples estimate reverse-time transport from C to B, and separately from B to A by direct application of (6) and FFT/IFFT transformation of the distributions. As in the FIT model, the components, u_1^* and u_2^*, are computed from the time series of the chemical observations at C, and also B in this case, which generates $\alpha_i(t)$. The mixing ratio function is then used in the deconvolution in conjunction with the TTDs estimated from (14). The FFT-based deconvolution was sensitive to the number of points used to discretize the time series functions but stable, consistent results were achieved with between 300-400 evenly spaced sample points; above this, the time series became oscillatory, obviously unstable, and consequently inaccurate.

The results of the BIT deconvolutions are shown in Figure 2b for the mixing ratios and Figure 3b, d, and f for the selected chemical species. The mixing ratio reconstruction of site B (Fig. 2b) is comparable to that observed in the FIT models. Inspecting Figure 3, we see some disagreement at early times in all three selected species for site A, though site B is well-approximated by the deconvolution. These errors are a combination of two factors: 1) insufficient temporal sampling of high frequencies for the FFT/IFFT, and 2) the inherent

smoothing of transfer functions. The former can be addressed somewhat by increasing the number of sample points but this can only be done up to the point where oscillatory behavior occurs as described above. The smoothing effect is largely unavoidable but when one considers the general Gaussian-like shape of the chemical curves in Fig 3b, d, and f, the approximation is still quite reasonable considering the simplicity of the numerical model.

5. Discussion

There are numerous additional details that could be explored like the role of errors, uncertainty, sampling errors, and numerical issues, among many others. These are important and merit more detailed investigation, but our main question centers singularly on whether or not it is possible to use transfer functions to approximate multi-component, mixing limited transport in this equilibrium reaction network. Our analysis shows that the approach works well in FIT and BIT applications, and we are unaware of any previous work that has explored these ideas. Beyond this, we offer a few noteworthy discussion points:

1. *Only the geochemical solution technique was simplified.* The conservative component approach may not be familiar to many readers, but it is just another way of representing the same reaction network. We have not changed the example carbonate system in any way, only the way it is solved. The component approach used here can be thought of as an alternative to globally implicit, or operator splitting schemes, but it still solves the same system. The main difference is that we expend effort simplifying the reaction equations, as opposed to discretizing them and integrating them over time.

2. *Components provide some level of built-in error checking.* Any system that is dominated by equilibrium reactions can help identify measurement errors. The laws of mass action require a precise balance of the contributing solutes and a simple evaluation of the equilibrium constant expressions using data collected from the field will reveal if there is significant error. Some small amount of error is likely to exist, but if the equilibrium constant is known, one can correct the observed concentrations using maximum likelihood estimation. Further, the method used to estimate TTDs is also sensitive to errors, but large errors are necessary to significantly impact the parameters of (14), and it is unlikely that different radiometric tracers will exhibit the same errors. We recommend *Cirpka et al.* [2007], *Massoudieh et al.* [2012], and *McCallum et al.* [2014] for more details on how the TTD estimation process can account for errors.

3. *Some amount of error should be expected in transport models.* It is important for any numerical method to exactly reproduce analytical examples. However, given uncertainties about the subsurface, it is unreasonable to expect that that a model will exactly reproduce real-world transport. A systematic, probabilistic study of the tradeoffs in uncertainty and error should be done to compare the "cost" of different methods, but our results show that a transfer functions can provide reasonable approximations when multi-component equilibrium reaction networks are involved.

4. *Transfer functions are not replacements for distributed parameter models.* Our intent with this note is not to dissuade or discourage practitioners from using DPMs, only to highlight that there are alternatives. Each technique has a fundamentally different purpose and unique limitations. For example, process-based DPMs may have better predictive capabilities after calibration than transfer functions, and also allow for even more complex

reaction models/mechanisms. However, each also has different sources of uncertainty and the best choice depends on the factors and goals of specific applications.

5. *Stationarity is limiting but generally unavoidable without additional information.* A transfer function is exact between two points with a known TTD, but any non-stationarities that are unaccounted will lead to inaccuracies. This relates to the previous point, but spatial changes cannot be identified without some kind of additional data (*i.e.* borehole, geochemical, geophysical, conceptual, etc...). Predictive transfer function models should be considered approximations but they afford first-order estimates of complex transport behaviors in the absence of more detailed data.

Convolutions and deconvolutions are not new and there are many other factors to consider for their application to transport problems. However, our focus is not on how to use transfer functions to model specific transport behaviors, rather it is on how to use complex reaction systems with transfer functions. We ask simply whether or not the workflow yields what could be called a reasonable approximation of the geochemistry in each case relative to the reference model. Given the approximation of $g(t)$, which was generated entirely from "observables," it should be clear that (1) works and (2) also performed well, overall. Here, a constant source model was used for the intruding fluid, but this was done only to keep the example simple; finite pulses also work in (2). Additional considerations will be needed for highly heterogeneous reactions, but these are also tractable as shown by *Romanov and Dreybrodt* [2006] and *Guadagnini et al.* [2009]. The mathematical framework and numerical evidence presented here shows that convolutions and deconvolutions may have untapped applications for modeling complex

geochemical transport, but experimental and field validation should still be explored in the future, along with analyses of tradeoffs in error, uncertainty, and model complexity.

Acknowledgments. This work was partially supported by the U.S. Department of Energy, Office of Science, Office of Biological and Environmental Research, under award number DE-SC0019123, and partially supported by the National Science Foundation under grant 1707753. Any opinions, findings and conclusions, or recommendations expressed in this material are those of the authors and do not necessarily reflect those of the NSF. The data presented in this note can be generated from the included equations.

Appendix A: Additional details for the geochemical system

Most of the details of the conservative component and mixing ratios approach are provided in section 3 but two necessary elements are also included here. The detailed foundations of this solution technique can be found in *Ginn et al.* [2017], who also corrected some inaccuracies in the previous work. Two notable changes are: 1) Eq. 22b of *de Simoni et al.* [2007] is incorrect, but can be corrected by replacing their K^* with $1/K^*$, and 2) our Eq. (A4) is an alternative form of the 6th order polynomial given as Eq. 22a by *de Simoni et al.* [2007]. Lastly, for completeness we provide the complete speciation of the two end-members used throughout this note in Table 1, and the reference model values of the radiometric tracers in Table 2.

A1. Stoichiometric matrix

The stoichiometric matrix $\mathbf{S}$ is used to speciate the secondary species from the primaries and is defined based on the full reaction system (8). The general formulation of the matrix

399 is given by *de Simoni et al.* [2007], but in this case the matrix is:

$$\mathbf{S} = \begin{bmatrix} 1 & -1 \\ 1 & -2 \\ -1 & 2 \\ 0 & -1 \end{bmatrix} \tag{A1}$$

A2. Equilibrium constant corrections

400 The values for K_{1-4} given in the text (following Eq. 8) are the standard reference values
401 of the equilibrium constants but these must be adjusted for ionic strength, which affects
402 the activity of each species (primary and secondary). Following de Simoni (2007), the
403 activity coefficients are estimated using the *Helgeson and Kirkham* [1974] model:

$$\log \gamma_m = \beta I_s - \frac{z_m^2 \eta \sqrt{I_s}}{1 + \xi a_m \sqrt{I_s}} \tag{A2}$$

404 where z_m is the valence of the mth species, a_m is the ionic radius (values given by *de*
405 *Simoni et al.* [2007]), $\eta = 0.5092$, $\xi = 0.3282$, and $\beta = 0.041$. Note that this corrects
406 a sign error in the version of this equation presented in *de Simoni et al.* [2007]. Also
407 it also noted that while this equation is of similar form to the commonly used extended
408 Debye-Huckel model (*e.g.*, Eq. 4.13 in *Appelo and Postma* [2004]), the parameters have
409 different definitions and values, as the *Helgeson and Kirkham* [1974] model is designed to
410 include high temperature (up to 600C) and pressure (up to 6 bar) conditions. The vector
411 of corrected equilibrium constants is:

$$\mathbf{K}^* = \left[K_1 \frac{\gamma_{HCO_3^-} \gamma_{H^+}}{\gamma_{CO_2}},\ K_2 \frac{\gamma_{CO_3^{2-}} \gamma_{H^+}^2}{\gamma_{CO_2}},\ K_3 \frac{\gamma_{Ca^{2+}} \gamma_{CO_2}}{\gamma_{H^+}^2},\ K_4 \gamma_{OH^-} \gamma_{H^+} \right]^T \tag{A3}$$

A3. Primary species from components

412 Either end-member ($\alpha = 0$ or $\alpha = 1$) is already a uniquely defined solution because
413 both primary species are known; however, mixtures will shift the equilibrium state. The
414 composition of the system will be a linear mixture of the conservative components, but

there is a nonlinear relationship between the concentrations in the equilibrated mixture. In order to speciate the system (via 9) the concentrations of the primary species must be found. Combining equations (11a) and (11b), we obtain the nonlinear (implicit) function for H^+:

$$u_1^* = -\frac{(H^+)^2(2K_1^*H^+ + 1)}{K_3^*\left[\frac{K_1^*}{K_4^*} - K_1^*(H^+)^2 + K_1^*H^+\Omega\right]} + \frac{\left[\frac{1}{K_1^*H^+} + \frac{1}{K_2^*(H^+)^2} + 1\right]\left[\frac{K_1^*}{K_4^*} - K_1^*(H^+)^2 + K_1^*\Omega H^+\right]}{2K_1^*H^+ + 1} \tag{A4}$$

where $\Omega = (2u_1^* + u_2^*)$, u_i^* are the mixed components (see Eq. 11), and K_i^* denote the equilibrium constants corrected for non-unit activity from (A3). The values of u_1 and u_2 are given by the mixing ration, α, and the and the equilibrium constants are known so the equation can be solved for H^+ using Newton iteration. With H^+, the concentration of CO_2 can then be found exactly from:

$$CO_{2,\alpha} = \frac{K_1^*\left[2H^+K_4^*u_1^* - (H^+)^2K_4^* + H^+K_4^*u_2 + 1\right]}{K_4^*(2H^+K_1^* + 1)} \tag{A5}$$

where the subscript α reminds us that this is conditional to a specific mixing ratio.

References

Alikhani, J., A. L. Deinhart, A. Visser, R. K. Bibby, R. Purtschert, J. E. Moran, A. Massoudieh, and B. K. Esser (2016), Nitrate vulnerability projections from bayesian inference of multiple groundwater age tracers, *Journal of Hydrology*, *543*, 167 – 181, doi:10.1016/j.jhydrol.2016.04.028.

Appelo, C. A., and D. Postma (2004), *Geochemistry, groundwater and pollution, second edition*, doi:10.1201/9781439833544.

Beisman, J. J., R. M. Maxwell, A. K. Navarre-Sitchler, C. I. Steefel, and S. Molins (2015), ParCrunchFlow: an efficient, parallel reactive transport simulation tool for physically and chemically heterogeneous saturated subsurface environments, *Computational Geosciences*, *19*, 403–422, doi:10.1007/s10596-015-9475-x.

Benettin, P., A. Rinaldo, and G. Botter (2013), Kinematics of age mixing in advection-dispersion models, *Water Resources Research*, *49*(12), 8539–8551, doi:10.1002/2013WR014708.

Bethke, C. M. (2007), *Geochemical and biogeochemical reaction modeling: Second edition*, doi:10.1017/CBO9780511619670.

Botter, G., E. Bertuzzo, A. Bellin, and A. Rinaldo (2005), On the Lagrangian formulations of reactive solute transport in the hydrologic response, *Water Resources Research*, doi:10.1029/2004WR003544.

Chiogna, G., O. A. Cirpka, P. Grathwohl, and M. Rolle (2011), Relevance of local compound-specific transverse dispersion for conservative and reactive mixing in heterogeneous porous media, *Water Resources Research*, *47*(7), doi:10.1029/2010WR010270.

Cirpka, O. A., and P. K. Kitanidis (2000), Characterization of mixing and dilution in heterogeneous aquifers by means of local temporal moments, *Water Resources Research*, *36*(5), 1221–1236.

Cirpka, O. A., and P. K. Kitanidis (2001), Transport of volatile compounds in porous media in the presence of a trapped gas phase, *Journal of Contaminant Hydrology*.

Cirpka, O. A., M. N. Fienen, M. Hofer, E. Hoehn, A. Tessarini, R. Kipfer, and P. K. Kitanidis (2007), Analyzing bank filtration by deconvoluting time series of electric conductivity., *Ground water*, *45*(3), 318–28, doi:10.1111/j.1745-6584.2006.00293.x.

Cook, P. G., and J. K. Böhlke (2000), Determining timescales for groundwater flow and solute transport, in *Environmental tracers in subsurface hydrology*.

Cvetkovic, V., G. Dagan, and H. Cheng (1998), Contaminant transport in aquifers with spatially variable hydraulic and sorption properties, *Proceedings of the Royal Society A: Mathematical, Physical and Engineering Sciences*, *454*(1976), 2173–2207, doi:10.1098/rspa.1998.0254.

de Simoni, M., X. Sanchez-Vila, J. Carrera, and M. W. Saaltink (2007), A mixing ratios-based formulation for multicomponent reactive transport, *Water Resources Research*, *43*(7), doi:10.1029/2006WR005256.

Dentz, M., T. Le Borgne, A. Englert, and B. Bijeljic (2011), Mixing, spreading and reaction in heterogeneous media: a brief review., *Journal of Contaminant Hydrology*, *120-121*, 1–17, doi:10.1016/j.jconhyd.2010.05.002.

Engdahl, N. B. (2014), Equivalence of the time and Laplace domain solutions for the steady state concentration of radiometric tracers and the groundwater age equation, *Water Resources Research*, *50*(4), 3602–3607, doi:10.1002/2014WR015413.

Engdahl, N. B., and R. M. Maxwell (2014), Approximating groundwater age distributions using simple streamtube models and multiple tracers, *Advances in Water Resources*, *66*, 19–31, doi:10.1016/j.advwatres.2014.02.001.

Engdahl, N. B., T. R. Ginn, and G. E. Fogg (2013), Using groundwater age distributions to estimate the effective parameters of Fickian and non-Fickian models of solute transport, *Advances in Water Resources*, *54*, 11–21, doi:10.1016/j.advwatres.2012.12.008.

Engdahl, N. B., D. A. Benson, and D. Bolster (2017), Lagrangian simulation of mixing and reactions in complex geochemical systems, *Water Resources Research*, *53*, 1–10,

477 doi:10.1002/2017WR020362.

478 Fienen, M. N., J. Luo, and P. K. Kitanidis (2006), A Bayesian geostatistical
479 transfer function approach to tracer test analysis, *Water Resources Research*, doi:
480 10.1029/2005WR004576.

481 Gardner, W. P., G. Hammond, and P. Lichtner (2015), High Performance Simulation
482 of Environmental Tracers in Heterogeneous Domains, *Ground Water*, *53*, 71–80, doi:
483 10.1111/gwat.12148.

484 Ginn, T. R. (2001), Stochastic-convective transport with nonlinear reactions and mixing:
485 finite streamtube ensemble formulation for multicomponent reaction systems with intra-
486 streamtube dispersion., *Journal of contaminant hydrology*, *47*(1), 1–28.

487 Ginn, T. R., E. M. Murphy, A. Chilakapati, and U. Seeboonruang (2001), Stochastic-
488 convective transport with nonlinear reaction and mixing: application to intermediate-
489 scale experiments in aerobic biodegradation in saturated porous media., *Journal of*
490 *Contaminant Hydrology*, *48*(1-2), 121–49.

491 Ginn, T. R., H. Haeri, A. Massoudieh, and L. Foglia (2009), Notes on groundwater age
492 in forward and inverse modeling, *Transport in Porous Media*, *79*(1), 117–134, doi:
493 10.1007/s11242-009-9406-1.

494 Ginn, T. R., L. G. Schreyer, X. Sanchez-Vila, M. K. Nassar, A. A. Ali, and S. Kräutle
495 (2017), Revisiting the Analytical Solution Approach to Mixing-Limited Equilibrium
496 Multicomponent Reactive Transport Using Mixing Ratios: Identification of Basis, Fix-
497 ing an Error, and Dealing With Multiple Minerals, *Water Resources Research*, *53*(11),
498 9941–9959, doi:10.1002/2017WR020759.

Gooseff, M. N., D. A. Benson, M. A. Briggs, M. Weaver, W. Wollheim, B. Peterson, and C. S. Hopkinson (2011), Residence time distributions in surface transient storage zones in streams: Estimation via signal deconvolution, *Water Resources Research*, *47*(5), 1–7, doi:10.1029/2010WR009959.

Green, C. T., B. C. Jurgens, Y. Zhang, J. J. Starn, M. J. Singleton, and B. K. Esser (2016), Regional oxygen reduction and denitrification rates in groundwater from multi-model residence time distributions, San Joaquin Valley, USA, *Journal of Hydrology*, *543*, 155 – 166, doi:10.1016/j.jhydrol.2016.05.018.

Green, C. T., L. Liao, B. T. Nolan, P. F. Juckem, C. L. Shope, A. J. Tesoriero, and B. C. Jurgens (2018), Regional Variability of Nitrate Fluxes in the Unsaturated Zone and Groundwater, Wisconsin, USA, *Water Resources Research*, doi: 10.1002/2017WR022012.

Guadagnini, A., X. Sanchez-Vila, M. W. Saaltink, M. Bussini, and B. Berkowitz (2009), Application of a mixing-ratios based formulation to model mixing-driven dissolution experiments, *Advances in Water Resources*, *32*, 756–766, doi: 10.1016/j.advwatres.2008.07.005.

Hammond, G. E., P. C. Lichtner, and R. T. Mills (2014), Evaluating the performance of parallel subsurface simulators: An illustrative example with PFLOTRAN, *Water Resources Research*, *50*(1), 208–228, doi:10.1002/2012WR013483.

Harman, C. J., D. M. Reeves, B. Baeumer, and M. Sivapalan (2010), A subordinated kinematic wave equation for heavy-tailed flow responses from heterogeneous hillslopes, *Journal of Geophysical Research*, *115*, F00A08, doi:10.1029/2009JF001273.

Helgeson, H. C., and D. H. Kirkham (1974), Theoretical prediction of the thermodynamic behaviour of aqueous electrolytes at high pressure and temperature: II Debye-Huckel parameters for activity coefficients and relative partial molo properties, *American Journal of Science*, *274*.

Jury, W. A. (1982), Simulation of solute transport using a transfer function model, *Water Resources Research*, *18*(2), 363–368, doi:10.1029/WR018i002p00363.

Kirchner, J. W., X. Feng, and C. Neal (2001), Catchment-scale advection and dispersion as a mechanism for fractal scaling in stream tracer concentrations, *Journal of Hydrology*, *254*(1-4), 82–101, doi:10.1016/S0022-1694(01)00487-5.

Liao, Z., D. Lemke, K. Osenbrück, and O. A. Cirpka (2013), Modeling and inverting reactive stream tracers undergoing two-site sorption and decay in the hyporheic zone, *Water Resources Research*, *49*(6), 3406–3422, doi:10.1002/wrcr.20276.

Loschko, M., T. Wöhling, D. L. Rudolph, and O. A. Cirpka (2016), Cumulative relative reactivity: A concept for modeling aquifer-scale reactive transport, *Water Resources Research*, *52*(10), 8117–8137, doi:10.1002/2016WR019080.

Luo, J., and O. A. Cirpka (2008), Traveltime-based descriptions of transport and mixing in heterogeneous domains, *Water Resources Research*, *44*(9), W09,407, doi:10.1029/2007WR006035.

Luo, J., M. Dentz, J. Carrera, and P. Kitanidis (2008), Effective reaction parameters for mixing controlled reactions in heterogeneous media, *Water Resources Research*, *44*(2), 1–12, doi:10.1029/2006WR005658.

Małoszewski, P., and A. Zuber (1982), Determining the turnover time of groundwater systems with the aid of environmental tracers, *Journal of Hydrology*, *57*(3-4), 207–231,

544 doi:10.1016/0022-1694(82)90147-0.

545 Massoudieh, A., and T. R. Ginn (2011), The theoretical relation between unsta-
546 ble solutes and groundwater age, *Water Resources Research*, *47*(10), 1–6, doi:
547 10.1029/2010WR010039.

548 Massoudieh, A., S. Sharifi, and D. K. Solomon (2012), Bayesian evaluation of groundwater
549 age distribution using radioactive tracers and anthropogenic chemicals, *Water Resources*
550 *Research*, *48*(9), 1–19, doi:10.1029/2012WR011815.

551 McCallum, J., N. Engdahl, T. Ginn, and P. Cook (2014), Nonparametric estimation
552 of groundwater residence time distributions: What can environmental tracer data
553 tell us about groundwater residence time?, *Water Resources Research*, *50*(3), doi:
554 10.1002/2013WR014974.

555 Parkhurst, D. L., and L. Wissmeier (2015), PhreeqcRM: A reaction module for transport
556 simulators based on the geochemical model PHREEQC, *Advances in Water Resources*,
557 *83*, 176–189, doi:10.1016/j.advwatres.2015.06.001.

558 Parkhurst, D. L., K. Kipp, P. Engesgaard, and S. R. Charlton (2004), PHAST - A program
559 for simulating ground-water flow, solute transport, and multicomponent geochemical
560 reactions, *USGS Techniques and Methods 6*, U.S. Geological Survey.

561 Payn, R. A., M. N. Gooseff, D. A. Benson, O. A. Cirpka, J. P. Zarnetske, W. B. Bow-
562 den, J. P. McNamara, and J. H. Bradford (2008), Comparison of instantaneous and
563 constant-rate stream tracer experiments through non-parametric analysis of residence
564 time distributions, *Water Resources Research*, *44*(6), doi:10.1029/2007WR006274.

565 Prommer, H., D. A. Barry, and C. Zheng (2003), MODFLOW/MT3DMS-based reactive
566 multicomponent transport modeling, doi:10.1111/j.1745-6584.2003.tb02588.x.

Romanov, D., and W. Dreybrodt (2006), Evolution of porosity in the saltwater-freshwater mixing zone of coastal carbonate aquifers: An alternative modelling approach, *Journal of Hydrology*, *329*(3-4), 661–673, doi:10.1016/j.jhydrol.2006.03.030.

Sanz-Prat, A., C. Lu, M. Finkel, and O. a. Cirpka (2015), On the Validity of Travel-Time Based Nonlinear Bioreactive Transport Models in Steady-State Flow, *Journal of Contaminant Hydrology*, *175-176*, 26–43, doi:10.1016/j.jconhyd.2015.02.003.

Sardin, M., D. Schweich, F. J. Leij, and M. T. van Genuchten (1991), Modeling the Nonequilibrium Transport of Linearly Interacting Solutes in Porous Media: A Review, *Water Resources Research*, *27*(9), 2287–2307, doi:10.1029/91WR01034.

Seeboonruang, U., and T. R. Ginn (2006), Upscaling heterogeneity in aquifer reactivity via the exposure-time concept : Inverse model, *Journal of Contaminant Hydrology*, *84*, 155–177, doi:10.1016/j.jconhyd.2005.12.010.

Simmons, C. S. (1982), A stochastic-convective transport representation of dispersion in one-dimensional porous media systems, *Water Resources Research*, *18*(4), 1193–1214, doi:10.1029/WR018i004p01193.

Simmons, C. S., T. R. Ginn, and B. D. Wood (1995), Stochastic-convective transport with nonlinear reaction: Mathematical framework, *Water Resources Research*, *31*(11), 2675–2688.

Steefel, C., and A. Lasaga (1994), A Coupled Model for Transport of Multiple Chemical Species and Kinetic Precipitation/Dissolution Reactions with Application to Reactive Flow in Single Phase Hydrothermal Systems, *American Journal of Science*, *294*, 529–592.

589 Steefel, C. I., and K. T. B. MacQuarrie (1996), Approaches to modeling of re-
590 active transport in porous media, *Reviews in Mineralogy and Geochemistry*, doi:
591 10.1080/07351692509349138.

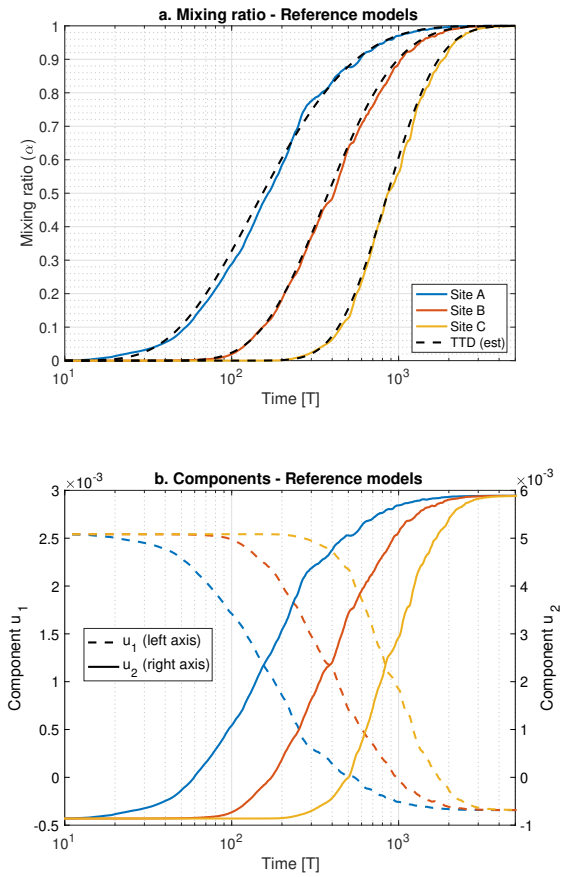

Figure 1. a) Mixing ratios at sites A, B, and C (denoted by color) for the reference model (solid lines), and b) the conservative components u_1 (left axis) and u_2 (right axis). The dashed black lines in panel "a" are the travel time distributions inferred from the radiometric tracers, ^{39}Ar and ^{3}H, which provide good approximations of these distributions. Some values of u_2 are negative, but this is permissible since it is a component, not a solute.

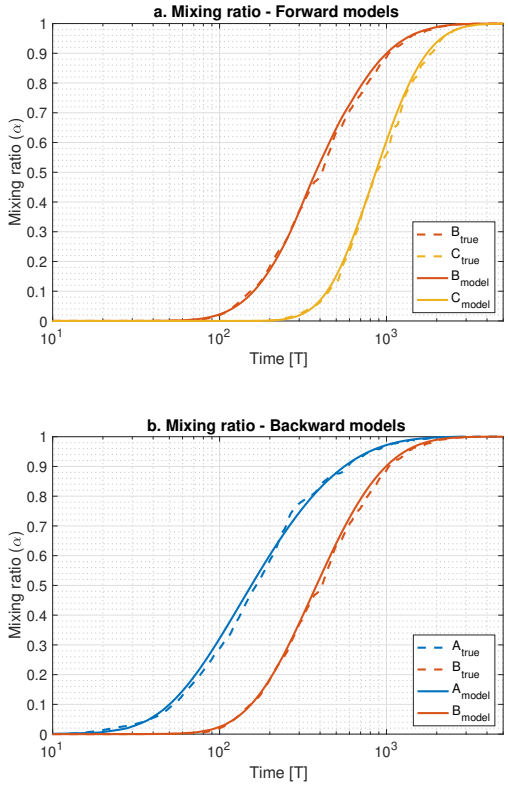

Figure 2. Transfer function estimated mixing ratios for a) the FIT models from Site A to B and C, and b) the BIT models from site C to B and from site B to A, respectively. Solid lines are the simulated (FIT and BIT) models and the dashed lines are the reference model. The smoothed TTD model and coarse discretization of the discrete FFT remove some of the noise, but the approximation is good overall.

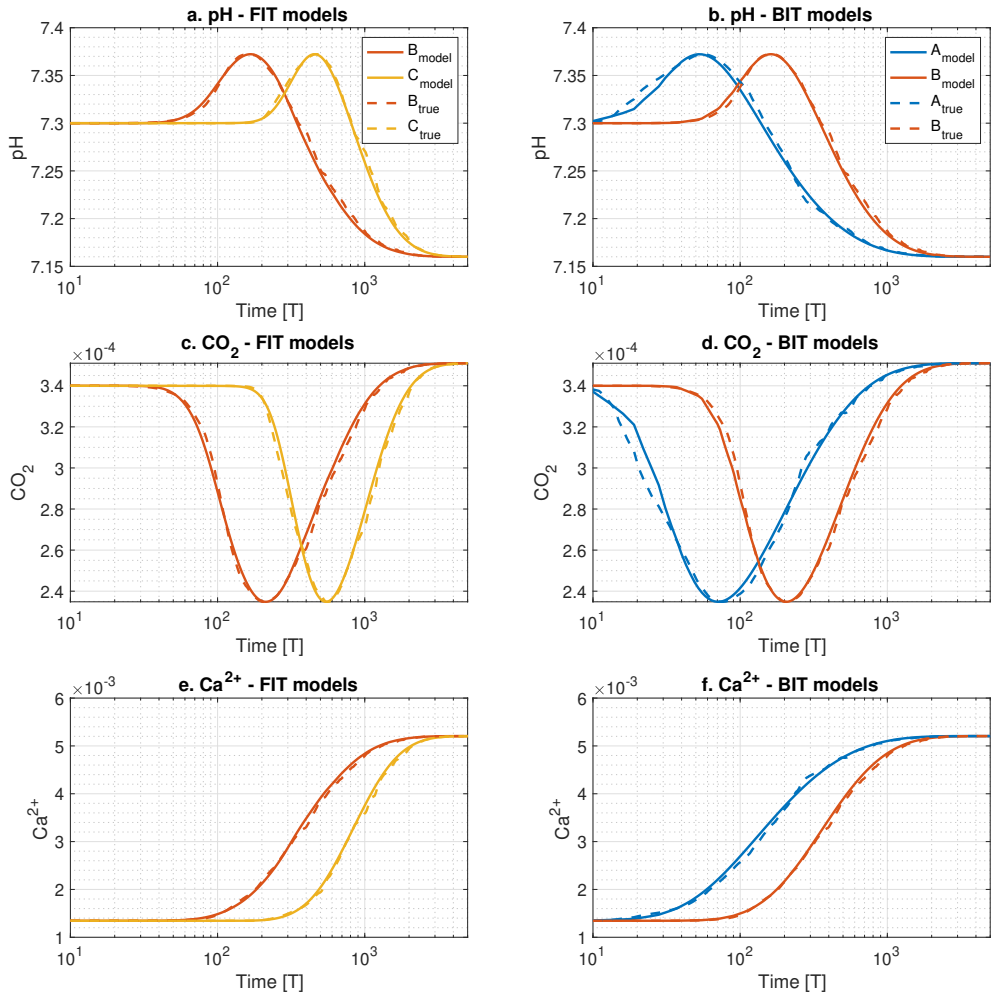

Figure 3. Selected, simulated solute concentrations for the FIT models from site A to B and C (panels a, c, and e), and b) the BIT models from site C to B and from B to A, respectively (panels b, d, and f). Solid lines are the transfer function models (FIT and BIT) and the dashed lines are the reference model. The coarse FFT discretization affected the IFFT for the BIT model resulting in some noticeable errors for the Site A reconstruction, but the signal is still approximated well.

Table 1. Complete speciation of the two end-member solutions used in the reactive transport system. I_s denotes ionic strength.

	EM-A	EM-B
CO_2	3.40×10^{-4}	3.51×10^{-4}
H^+	5.01×10^{-8}	6.92×10^{-8}
HCO_3^-	3.54×10^{-3}	4.50×10^{-3}
CO_3^{2-}	4.43×10^{-6}	1.21×10^{-5}
Ca^{2+}	1.35×10^{-3}	5.21×10^{-3}
OH^-	2.31×10^{-7}	2.86×10^{-7}
I_s	5.00×10^{-3}	6.25×10^{-1}

Table 2. Normalized, reference model concentrations of the radiometric tracers used to estimate the TTD parameters in (14)

	Site A	Site B	Site C
^{39}Ar	9.21×10^{-1}	8.48×10^{-1}	7.72×10^{-1}
^{3}H	3.35×10^{-1}	1.13×10^{-1}	1.27×10^{-2}